Roberto Caudana, MD • Giovanni Morana, MD • Gian Paolo Pirovano, MD • Nicola Nicoli, MD
Antonella Portuese, MD • Alberto Spinazzi, MD • Rosa Di Rito, MD • Gian Franco Pistolesi, MD

Focal Malignant Hepatic Lesions: MR Imaging Enhanced with Gadolinium Benzyloxypropionictetra- acetate (BOPTA)—Preliminary Results of Phase II Clinical Application[1]

PURPOSE: **To investigate enhancement with gadolinium benzyloxypropionictetraacetate (BOPTA) at magnetic resonance (MR) imaging to detect focal malignant hepatic lesions.**

MATERIALS AND METHODS: **A phase II trial was performed in 34 patients. Gd-BOPTA-enhanced spin-echo (SE) and gradient-recalled-echo (GRE) T1-weighted MR imaging were performed at 40 and 90 minutes after intravenous injection of 0.05 and 0.10 mmol/kg Gd-BOPTA.**

RESULTS: **The percentage of enhancement in liver parenchyma was significantly ($P < .05$) increased on GRE T1-weighted compared with SE T1-weighted images at 40 and 90 minutes after injection of the higher dose and compared with SE and GRE T1-weighted images obtained with the lower dose. The contrast-to-noise ratio of metastases was significantly increased on GRE T1-weighted images (0.10 mmol/kg) at 90 minutes compared with precontrast images. Significantly more small primary metastases were detected on GRE T1-weighted images (0.10 mmol/kg) at 90 minutes compared with precontrast SE T1-weighted images.**

CONCLUSION: **Gd-BOPTA is a safe hepatobiliary contrast agent that helps detection of small metastases.**

Index terms: Contrast media, 761.12143 • Gadolinium, 761.12143 • Liver, MR, 761.12143 • Liver neoplasms, MR, 761.33 • Magnetic resonance (MR), contrast agents, 761.12143

Radiology 1996; 199:513–520

UNENHANCED magnetic resonance (MR) imaging of focal malignant hepatic lesions provides little improvement compared with contrast material–enhanced computed tomography (CT) with dynamic and/or delayed evaluation (1–4); moreover, the sensitivity of MR imaging is inferior to that of CT during arterial portography (85%–91%) (4,5). One approach to improving the sensitivity of MR imaging to intrahepatic lesions has been to develop hepatobiliary-specific contrast agents (6–14). Among the hepatobiliary contrast materials, gadolinium benzyloxypropionictetraacetate (BOPTA) showed high hepatobiliary excretion in in vivo studies in rats (38.6%) (15,16) and a fairly poor hepatobiliary excretion in humans (2%–4%) (17). In a preliminary study of eight healthy male volunteers, the tolerability and efficacy of Gd-BOPTA in providing enhancement in the liver were assessed (18). In this article, we describe enhancement with Gd-BOPTA in the identification of focal hepatic malignancies.

MATERIALS AND METHODS

Contrast Agent

Gd-BOPTA is an octadentate chelate of gadolinium supplied by Bracco (Milan, Italy). The synthesis and stability and constant and relaxivity values of Gd-BOPTA have been described previously (15,19,20). The contrast agent was formulated in two concentrations (0.25 and 0.5 mmol/L). The density and osmolality values of the 0.5-mmol/L solution are comparable to those for 0.5-mmol/L gadopentetate dimeglumine (Magnevist; Schering, Berlin, Germany), whereas the values of the 0.25-mmol/L solution are obviously below those of 0.5-mmol/L gadopentetate dimeglumine. Injections were performed outside the magnet room, with the patients in a comfortable position. The intravenous administration rate was approximately 10 mL/min.

Study Design

The study protocol was designed to assess safety, tolerance, and efficacy of two different dose levels (0.05 and 0.10 mmol per kilogram of body weight) of Gd-BOPTA; this protocol underwent preliminary approval by the ethics committee of our institution. Patient exclusion criteria included age less than 18 years or greater than 75 years, known reactions after the administration of gadolinium compounds, injection with either iodinated contrast agents during the preceding 48 hours or of gadolinium compounds in the past 30 days, pregnancy, cardiovascular failure, severe liver and renal failure, and known contraindications to the MR imaging examination.

Thirty-four patients (12 women, 22 men, aged 25–75 years [mean, 58.6 years ± 12.2 [standard deviation]]) were selected to participate in this study on the basis of focal hepatic lesions depicted at transabdominal ultrasonography (US) and/or CT. All CT examinations were performed with conventional scanners (DR series; Siemens, Erlangen, Germany) with 8-mm-thick contiguous sections, 125 kVp, 230 mA, and a 3-second scanning time. CT was performed before and during administration of 150 mL nonionic contrast media at a concentration of 350 mg iodine per milliliter (Omnipaque 350; Nycomed Imaging, Oslo, Norway) or 370 mg iodine per milliliter (Iopamine 370; Bracco), with a dedicated injector (MedRad, Pittsburgh, Pa), at an injection rate of 2 mL/sec.

MR imaging was performed after injection of Gd-BOPTA was randomly administered at two dose levels. The first group (16 patients [eight men and eight women, aged 25–75 years [mean, 57.8 years ± 15.2]]) received 0.10 mL/kg of the 0.25 mmol/L Gd-BOPTA solution, which corresponds to a dose of 0.05 mmol/kg. The second group (18 patients [14 men and four women, aged 33–72 years [mean, 59.3 years ± 9.2]]) received 0.10 mL/kg of the 0.5 mmol/L Gd-BOPTA solution, which corresponds to a dose of 0.10 mmol/kg. These doses were demonstrated to be

[1] From the Departments of Radiology (R.C., G.M., A.P., R.D.R., G.F.P.) and Surgery (N.N.), University of Verona, Via delle Menegone, 37134 Verona, Italy; and Bracco S. p. A., Milan, Italy (G.P.P., A.S.). Supported totally by a grant from Bracco. Received November 1, 1995; revision requested December 12; revision received January 24, 1996; accepted January 26. **Address reprint requests to** R.C.

Abbreviations: BOPTA = benzyloxypropionictetraacetate, CI = confidence interval, C/N = contrast-to-noise ratio, EOB-DTPA = 4(S)-4-(4-ethoxybenzyl)-3,6,9-tris(carboxylatomethyl)-3,6,9-triazaundecandioic acid–disodium salt, GRE = gradient-recalled-echo, SE = spin echo.

optimal for liver MR imaging by other investigators (18).

Clinical monitoring (physical examination, blood pressure measurement, electrocardiography, and blood and urine laboratory tests focused on potential cardiovascular, hematologic, renal, and hepatobiliary effects) was performed before and at 24 and 72 hours after injection of Gd-BOPTA. Any discomfort and/or laboratory test abnormality reported within 24 hours after injection of Gd-BOPTA was followed up to complete recovery.

In all patients, focal malignant lesions of the liver were confirmed with either fine-needle liver biopsy (n = 8) or histologic examination of the resected specimen (n = 26). Primary liver cancers were found in 21 patients (17 with hepatocellular carcinoma, four with cholangiocarcinoma). Among the patients with hepatocellular carcinoma, some had either cirrhosis (n = 5) or chronic hepatitis (n = 3). The degree of differentiation at histologic grading was poor (n = 6), moderate (n = 6), and well differentiated (n = 5). Metastases were found in 13 patients (colorectal adenocarcinoma in six, renal carcinoma in two, carcinoid tumor in two, pancreatic neuroendocrine tumor in two, and retroperitoneal sarcoma in one).

All patients underwent intraoperative US, inspection, and palpation; the findings at intraoperative US and surgical exploration were the standards of reference for the qualitative evaluations.

Enhancement of Liver Parenchyma on Gd-BOPTA-enhanced MR Images

Imaging Sequence and Dose (mmol/kg)	Time after Injection of Gd-BOPTA: 40 Minutes — Median Percentage of Enhancement	40 Minutes — Standard Deviation	90 Minutes — Median Percentage of Enhancement	90 Minutes — Standard Deviation
SE T1-weighted				
0.05	30	45	35	40
0.10	51	36	44	25
GRE T1-weighted				
0.05	44	30	47	59
0.10	83	36	86	35

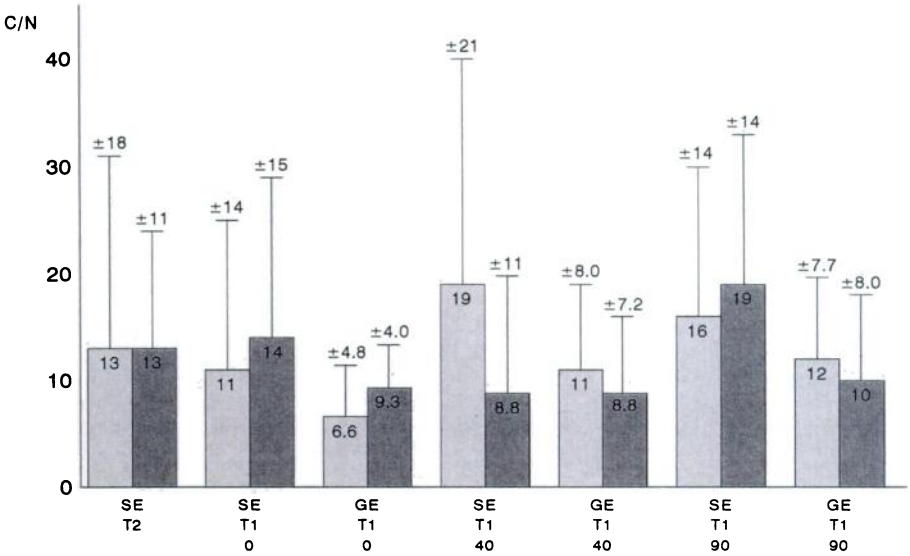

Figure 1. Primary malignant tumors (n = 21). Graph depicts median values (on bar) and standard deviations (above error bar) of the liver-to-lesion C/N on SE (*SE*) T2 (*T2*)-weighted images and on SE and GRE (*GE*) T1 (*T1*)-weighted images obtained before (*0*) and at 40 (*40*) and 90 (*90*) minutes after administration of the two doses (0.05 [gray bars] and 0.10 [black bars] mmol/kg) of Gd-BOPTA.

MR Imaging

MR imaging was performed on a 1.5-T superconducting clinical unit (Magnetom 63 SP; Siemens). The liver was evaluated with multisection acquisition; 10–14 transaxial sections (10-mm-thick sections, 2–4-mm gap) were obtained to examine the whole liver. Matrix values were reduced to decrease the acquisition time (144 × 256-pixel matrix with spin-echo [SE] sequences, 33 examinations; 160 × 256-pixel matrix with gradient-recalled-echo [GRE] sequences, 34 examinations; 192 × 256-pixel matrix with SE sequences, one examination). The field of view was changed according to the size of each patient (285 × 380 mm, five patients; 350 × 400 mm, 29 patients).

Before injection of Gd-BOPTA, MR imaging was performed with SE T1-weighted pulse sequences (repetition time msec/echo time msec = 350–550/15, with three or four signals acquired) and T2-weighted (1,800–2,000/15, 90; with 60° flip angle and two signals acquired). GRE T1-weighted pulse sequences (95/4, with 80° flip angle and one signal acquired) were performed in a single breath-hold interval of 20 seconds or less.

At 40 and 90 minutes after injection of Gd-BOPTA, MR imaging was performed with the same SE and GRE T1-weighted pulse sequences.

Analysis of Images

Quantitative analysis was performed, in an operator-defined region of interest, of the signal intensity and standard deviation of the liver and of a paramagnetic standard (nickel chloride), which was contained within two test tubes taped to the patient's abdomen. The signal intensity and standard deviation of the background were also measured. A region of interest of the same size was used in all imaging examinations performed in a patient. In the liver, the signal intensity was measured either within the normal parenchyma or within the lesion (in the largest mass if multiple lesions were present). For measurements within the lesion, the region of interest was positioned manually to avoid the necrotic foci; the signal intensity of the NiCl was also measured in the same image.

The percentage of enhancement (PE) of the signal intensity (SI) of the liver after (post) administration of Gd-BOPTA was calculated with SI of the liver and NiCl measured before (pre) and after (post) injection, according to the following formula (18): $PE = [(SI^{liver}_{post}/SI^{NiCl}_{post} - SI^{liver}_{pre}/SI^{NiCl}_{pre}) \div (SI^{liver}_{pre}/SI^{NiCl}_{pre})] \times 100$.

The contrast-to-noise ratio (C/N), which reflects the difference in signal intensity (SI) between the normal liver parenchyma and the lesion, was calculated according to the following formula (21): $C/N = (SI_{lesion} - SI_{liver}) \div SD_{background\ noise}$, where SD is standard deviation. The C/Ns of SE and GRE T1-weighted images are reported with positive values to ease the comparison with the median C/N measured in the precontrast SE T2-weighted images in the same series.

Statistical analysis (BMDP Statistical Software, Los Angeles, Calif) of the differences between the two doses of Gd-BOPTA in the percentage of enhancement at 40 and 90 minutes was performed with the Mann-Whitney *U* test. Statistical analysis of the differences in the C/Ns before and after administration of Gd-BOPTA was performed with the nonparametric Wilcoxon signed-rank test for matched pairs, with Bonferroni correction for multiple testing.

Qualitative analysis was performed by dividing the detectable lesions into three groups, on the basis of their diameter: 1 cm or less, 1–3 cm, more than 1–3 cm, and more than 3 cm. This analysis was performed by two blinded readers (R.C., G.M.) for both the CT and MR examinations and

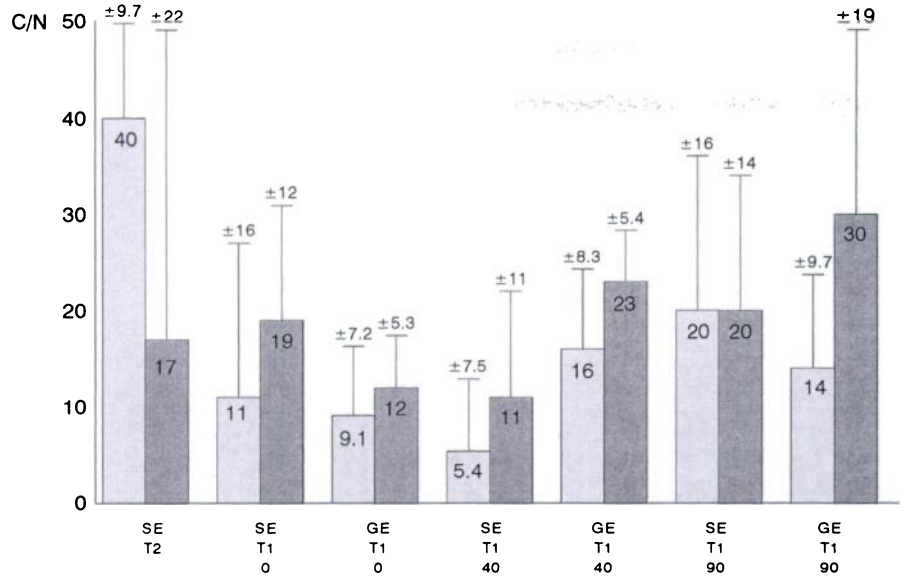

Figure 2. Metastases (n = 13). Graph depicts median values (on bar) and standard deviations (above error bar) of the liver-to-lesion C/N on SE (*SE*) T2 (*T2*)-weighted images and on SE and GRE (*GE*) T1 (*T1*)-weighted images obtained before (*0*) and at 40 (*40*) and 90 (*90*) minutes after administration of the two doses (0.05 [gray bars] and 0.10 [black bars] mmol/kg) of Gd-BOPTA.

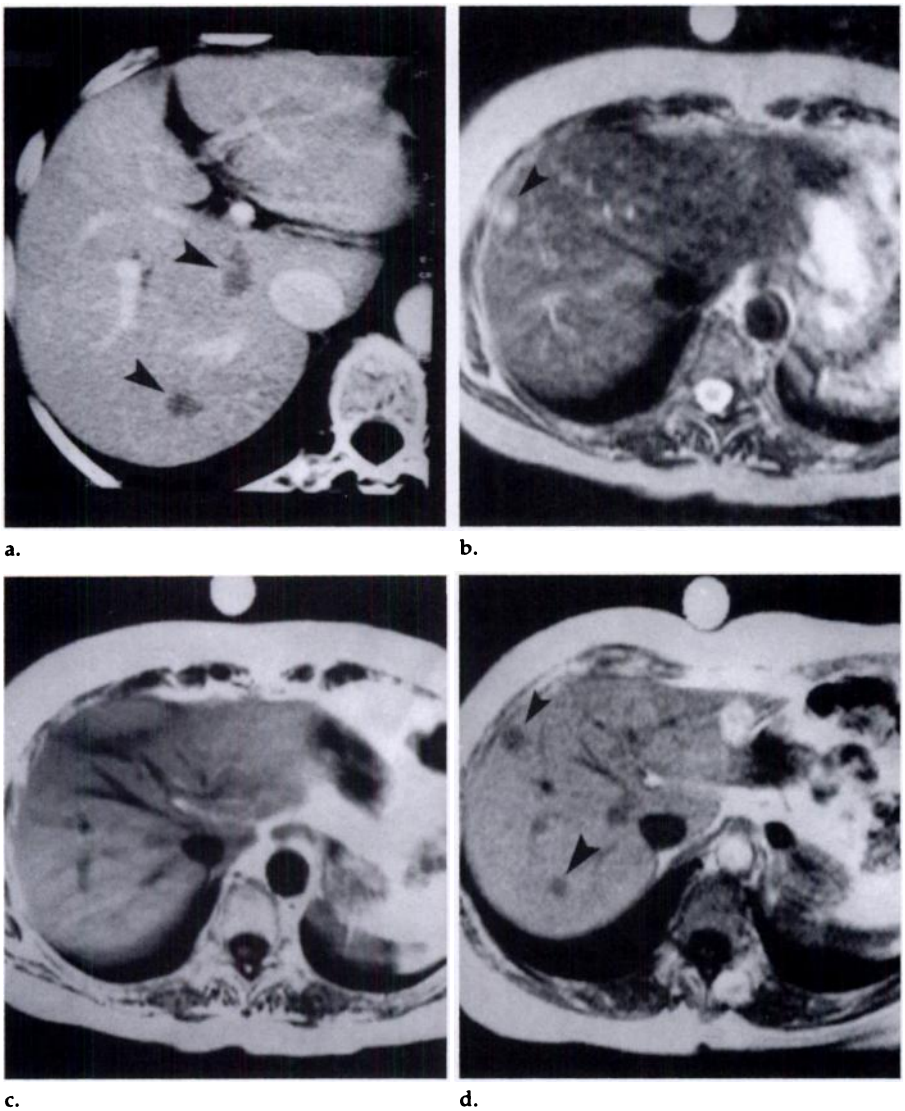

a. **b.** **c.** **d.**

Figure 3. Renal carcinoma with multiple liver metastases. **(a)** Contrast-enhanced CT scan. **(b–d)** MR images were obtained before injection of 0.10 mmol/kg Gd-BOPTA (*Fig 3 continues*).

for the two doses of Gd-BOPTA. All pre- and postcontrast MR images were seen at the same time by each reader. An initial interpretation was made independently, and differences in interpretation were later resolved by consensus; only the results of the consensus reading were considered in the final analysis. The evaluation of conspicuity and border definition of the lesion was performed before and after injection of contrast material to assess any improvement.

Qualitative analysis was performed by evaluating each multisection set of images obtained with each imaging sequence before (SE T1- and T2-weighted and GRE T1-weighted) and at 40 and 90 minutes after injection of Gd-BOPTA (SE and GRE T1-weighted). The standard of reference was established by a sonographer (A.P.) and a surgeon (N.N.), who agreed on a single final interpretation of the total number of lesions detected at intraoperative US during surgical exploration. This evaluation was performed without separating the detected lesions according to their size, owing to the difficulty of assessing the precise size of the lesions at intraoperative US or surgical inspection and palpation. Statistical analysis of the difference in the number of lesions counted on the various images obtained before and after administration of Gd-BOPTA, with both doses, was performed with the nonparametric Wilcoxon signed-rank test for matched pairs, with Bonferroni correction for multiple testing. A P value less than .05 was considered statistically significant. The same test was also used to assess the difference in the number of lesions detected with Gd-BOPTA-enhanced MR imaging, contrast-enhanced CT, and the standard of reference. Sensitivity levels with confidence intervals (CIs) were also calculated at contrast-enhanced CT and MR imaging before and after administration of Gd-BOPTA.

RESULTS

Patient Monitoring

No adverse side effects were observed during intravenous administration of Gd-BOPTA. A transient increase in blood pressure of 8.6 mm Hg plus or minus 6.9 and in pulse rate of 10.7 beats per minute plus or minus 7.4 immediately after the injection was observed that was believed to be caused by the injection; the increases did not persist, did not necessitate medical treatment, or were not considered serious by the investigators. One female patient with metastatic renal carcinoma, who received 0.10 mmol/kg Gd-BOPTA, experienced one episode of mild diarrhea 24 hours after injection that completely subsided within 72 hours after injection. No clinically important changes were observed at electrocardiography or in the blood and urine laboratory tests.

Quantitative Analysis

Percentage of enhancement.—The median values of the percentage of enhancement in the liver parenchyma after administration of the two doses of contrast material (0.05 and 0.10 mmol/kg) on T1-weighted SE and GRE images obtained at 40 minutes and 90 minutes after injection are reported in the Table. The highest percentages of enhancement in the hepatic tissue have been achieved with the higher dose of contrast material on GRE T1-weighted images obtained at 40 (83% ± 36) and 90 minutes (86% ± 35). The difference in percentage of enhancement at each time was not significant. Moreover, the percentage of enhancement on GRE T1-weighted images obtained with the higher dose was significantly superior to the percentage of enhancement on SE T1-weighted images obtained at both time points with either dose of contrast agent. On only GRE T1-weighted images was the difference significant ($P <$ .01) in the percentage of enhancement depicted on images obtained at both time points with both the lower dose (44% ± 30 at 40 minutes, 47% ± 59 at 90 minutes) and the higher dose (83% ± 36 at 40 minutes, 86% ± 35 at 90 minutes).

C/Ns.—The median C/Ns before and after administration of Gd-BOPTA are reported in Figures 1 and 2. As shown in Figure 1, the highest median C/N measured in the series of primary malignant lesions were achieved with the SE T1-weighted sequence at 40 minutes (19 ± 21) with the lower dose and at 90 minutes (19 ± 14) with the higher dose; at 40 minutes in images obtained with the same sequence, the C/N in the images obtained with the higher dose (8.8 ± 11.0) was low compared with the value at 40 minutes in images obtained with the lower dose (19 ± 21). No significant difference was observed in the C/Ns on pre- and postcontrast SE and GRE images or on images obtained with the two doses. The C/Ns measured on precontrast SE T2-weighted images were 13 ± 18 (0.05 mmol/kg dose) and 13 ± 11 (0.10 mmol/kg dose). No significant difference in C/Ns was observed on precontrast SE T2-weighted images and postcontrast SE and GRE T1-weighted images.

In Figure 2, the highest median C/Ns measured in this series of liver metastases were achieved on postcontrast SE T1-weighted images obtained at 90 minutes with 0.05 and 0.10 mmol/kg Gd-BOPTA (20 ± 16 and 20 ± 14, respectively) and on GRE T1-weighted images obtained at 90 minutes with 0.10 mmol/kg Gd-BOPTA (30 ± 19). A significant difference in C/N was observed between GRE T1-weighted images obtained before and at 90 minutes after injection of 0.10 mmol/kg Gd-BOPTA. The C/Ns measured on precontrast SE T2-weighted images were 40.0 plus or minus 9.7 (0.05 mmol/kg dose) and 17 plus or minus 22 (0.10 mmol/kg dose). No significant difference was observed between the C/Ns on precontrast SE T2-weighted images and on the GRE T1-weighted images obtained 90 minutes after intravenous administration of 0.10 mmol/kg Gd-BOPTA.

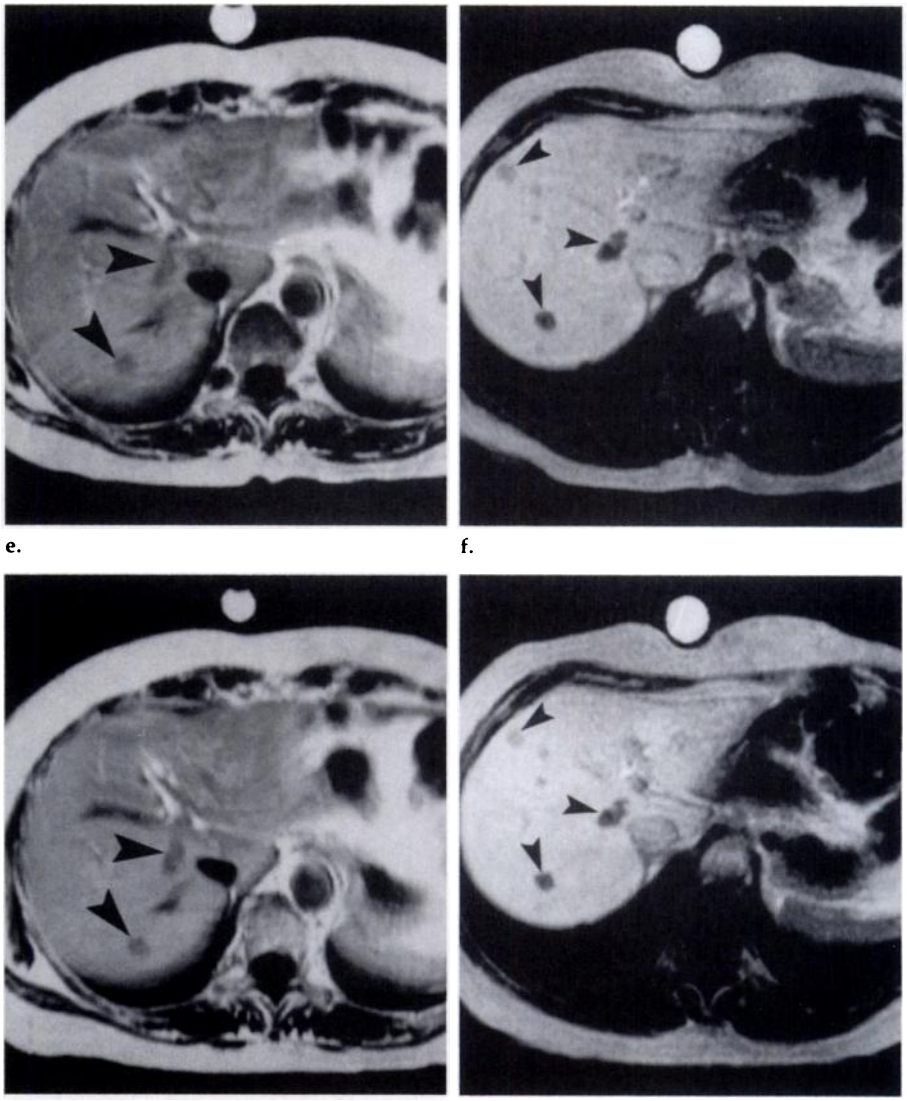

Figure 3 (*continued*). **(e–h)** MR images were obtained at 40 minutes (in **e**, **f**) and 90 minutes (in **g**, **h**) after injection of 0.10 mmol/kg Gd-BOPTA. The images were obtained with conventional SE T2-weighted (in **b**) and T1-weighted (in **c**, **e**, **g**) sequences and with a fast GRE T1-weighted sequence (in **d**, **f**, **h**). The enhancement in the liver parenchyma, the C/N, and the number of the lesions (arrowheads) that could be detected with confidence increased on **f** and **h**.

Qualitative Analysis

Improved conspicuity and definition of the lesion border was observed by both readers and was more pronounced in metastases (Fig 3) than in primary malignant lesions (Fig 4). Figures 5 and 6 show the number of lesions identified on contrast-enhanced CT scans and on pre- and postcontrast MR images, divided into the three size categories, as well as the sensitivity values.

Primary malignancies.—For primary malignancies (n = 21), the maximum number of lesions 1 cm or less in diameter (n = 37) (Fig 5) was detected on postcontrast GRE T1-weighted images at 40 minutes. The maximum number of lesions more than 1 cm to 3 cm in diameter (n = 16) was detected on precontrast SE T1-weighted images. The maximum number of lesions more than 3 cm in diameter (n = 19) was demonstrated on postcontrast

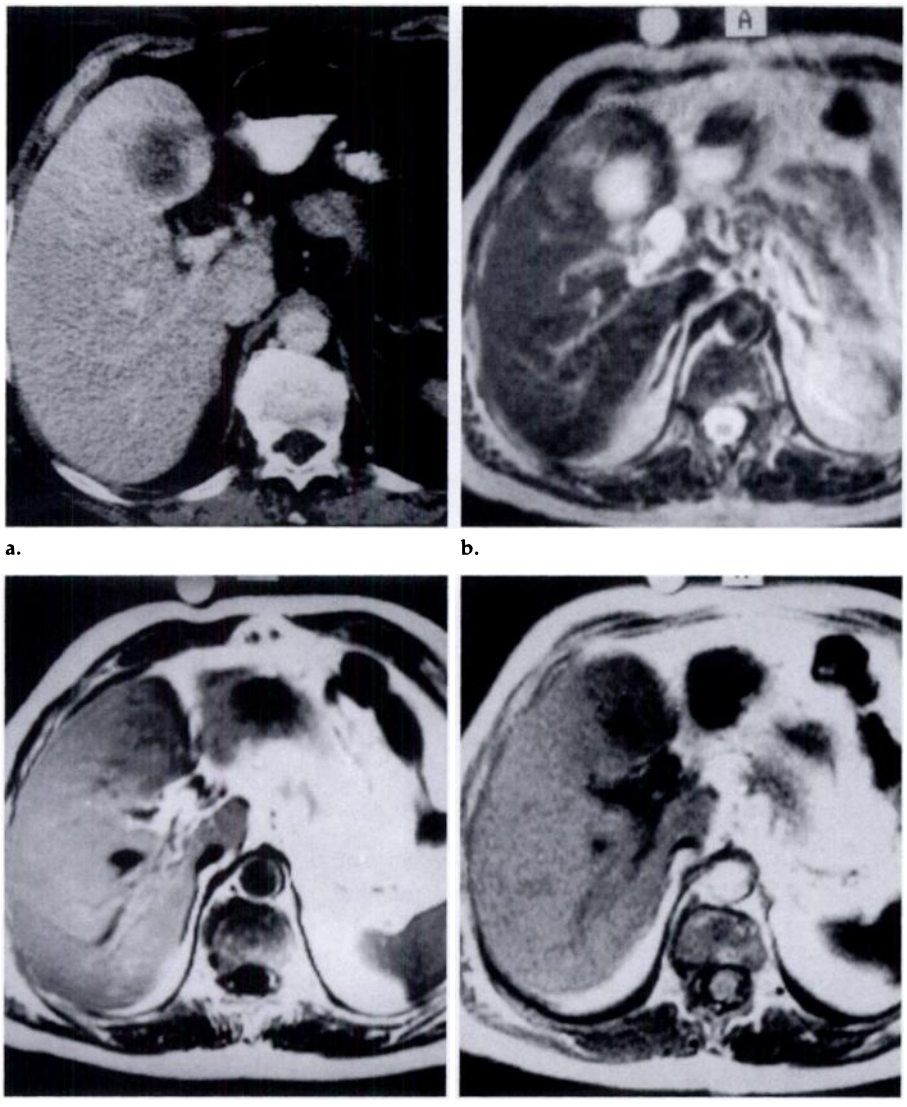

Figure 4. Cholangiocarcinoma of the fourth segment. **(a)** Contrast-enhanced CT scan. **(b–d)** MR images were obtained before injection of 0.10 mmol/kg Gd-BOPTA (*Fig 4 continues*).

GRE T1-weighted images obtained at 90 minutes. No significant difference was observed in the number of lesions 1 cm or less in diameter that were detected on images obtained with any of the unenhanced or contrast-enhanced MR imaging sequences or on contrast-enhanced CT scans. In a comparison of images obtained with all the unenhanced or contrast-enhanced MR imaging sequences, the difference between the total number of primary lesions detected on MR images compared with the standard of reference (n = 96) was significant for only SE T1-weighted images obtained before and at 40 minutes after injection of Gd-BOPTA. The sensitivity values and the CIs included the following: CT (0.68 [95% CI, 0.59, 0.77]); unenhanced MR imaging, SE T2-weighted (0.45 [95% CI, 0.36, 0.54), SE T1-weighted (0.32 [95% CI, 0.23, 0.41]), and GRE T1-weighted (0.43 [95% CI, 0.34, 0.52]); contrast-enhanced MR imaging, at 40 minutes after injection, SE T1-weighted (0.41 [95% CI, 0.32, 0.50]), GRE T1-weighted (0.71 [95% CI, 0.63, 0.79]), and at 90 minutes after injection, SE T1-weighted (0.52 [95% CI, 0.43, 0.61]) and GRE T1-weighted (0.72 [95% CI, 0.64, 0.80]).

Metastases.—In the series of metastases (n = 13), the maximum number of metastases not more than 1 cm in diameter (Fig 6) was detected on postcontrast GRE T1-weighted MR images obtained 90 minutes after injection of Gd-BOPTA (n = 158). The maximum number of lesions more than 1 cm to 3 cm in diameter was detected on postcontrast SE T1-weighted MR images obtained 90 minutes after injection of Gd-BOPTA (n = 91). Lesions more than 3 cm in diameter (n = 15) were detected equally on unenhanced and contrast-enhanced images obtained with all pulse sequences except on postcontrast SE T1-weighted images obtained at both 40 and 90 minutes after injection of Gd-BOPTA (n = 14). For lesions not more than 1 cm in diameter, the difference in the number of lesions detected was significant between only postcontrast GRE T1-weighted images obtained at 90 minutes and precontrast SE T1-weighted images. In a comparison of the number of metastases depicted on images obtained with all unenhanced and contrast-enhanced MR imaging sequences and the standard of reference (n = 285), the difference was significant for only precontrast SE T1-weighted images. The sensitivity values with CIs were the following: CT (0.52 [95% CI, 0.47, 0.57]); unenhanced MR imaging, SE T2-weighted (0.56 [95% CI, 0.51, 0.61]), SE T1-weighted (0.38 [95% CI, 0.33, 0.43]), and GRE T1-weighted (0.48 [95% CI, 0.43, 0.53]); contrast-enhanced MR imaging, at 40 minutes, SE T1-weighted imaging (0.44 [95% CI, 0.39, 0.49]) and GRE T1-weighted imaging (0.84 [95% CI, 0.80, 0.88]), and at 90 minutes, SE T1-weighted (0.62 [95% CI, 0.57, 0.67]) and GRE T1-weighted (0.89 [95% CI, 0.86, 0.92]).

DISCUSSION

Among the water-soluble paramagnetic contrast agents that influence the T1 relaxation time, those targeted to the hepatocytes are currently under investigation (22). Gd-BOPTA is excreted through both the urinary and hepatobiliary routes. The benzyloxymethyl group represents the molecular handle that enables Gd-BOPTA to be recognized by a carrier-mediated transport system and thus taken up by the hepatocyte; the biliary excretion of Gd-BOPTA was shown to be a saturable process and its hepatic clearance to be inhibited by bromosulfophtalein (18,23).

In the current study we confirmed an increased enhancement in the liver parenchyma after administration of Gd-BOPTA, which had already been observed by Vogl et al in healthy volunteers (18), that is due to the active transport mechanism of the contrast agent within the hepatocyte. A dose of 0.10 mmol/kg demonstrated significantly greater enhancement on GRE images obtained at both 40 and 90 minutes after injection. Similar values of liver enhancement with doses higher than 0.10 mmol/kg have been demonstrated previously in animals (16) and in humans (18). It is not known so far if the lack of further increase in the enhancement with doses

higher than 0.10 mmol/kg is due to saturation of the mechanism of the carrier-mediated cellular uptake or to an increased T2 effect (7,18).

Other positive paramagnetic contrast agents besides Gd-BOPTA accumulate within the liver tissue, including mangafodipir trisodium (Mn-DPDP) (6) and gadopentetate dimeglumine covalently linked to the lipophilic ethoxybenzyl moiety 4(S)-4-(4-ethoxybenzyl)-3,6,9-tris(carboxylatomethyl)-3,6,9-triazaundecandioic acid–disodium salt (Gd-EOB-DTPA) (12). Additionally, these hepatobiliary paramagnetic contrast materials increase the relaxivity of the hepatic tissue and thus the sensitivity of MR imaging for detection of intrahepatic tumors. The higher relaxivity of the hepatic tissue after administration of hepatobiliary-specific contrast agents is probably due to either an increased microviscosity inside the hepatocyte or to some transient interaction with intracellular proteins (22). Therefore, the surprising relaxivity of Gd-BOPTA within hepatic tissue (30 $[mmol/L \cdot sec]^{-1}$), which is higher than the relaxivity of mangafodipir trisodium (21.7 $[mmol/L \cdot sec]^{-1}$) and of Gd-EOB-DTPA (16.6 $[mmol/L \cdot sec]^{-1}$) in the same target tissue, may be related to the high macromolecular binding, which could compensate for the lower hepatocellular uptake of Gd-BOPTA compared with the significantly higher uptake of mangafodipir trisodium and Gd-EOB-DTPA (15,22).

Primary malignant lesions showed a wide variation in C/N after administration of Gd-BOPTA. No significant difference was found in the C/N of primary lesions before and after administration of Gd-BOPTA. This variation may be due to the interindividual variability (22) in liver function caused by age and liver diseases (hepatitis, cirrhosis, tumor spread), which may reduce the amount of contrast material uptake by the hepatocytes. It is likely that the saturation of hepatocytic uptake is reached more rapidly with the higher dose (0.10 mmol/kg) of Gd-BOPTA.

As to the behavior of the lesion, tumor enhancement is affected not only by the early and short vascular and interstitial phase of Gd-BOPTA but also by the pooling of contrast material in the central, less vascularized area of the tumor, where the rate of washout is decreased (24). In addition, the tumors in the four cases of cholangiocarcinoma were large (diameter, 6–10 cm); thus, it is likely that the delayed washout of Gd-BOPTA in these lesions reduced the difference in signal intensity compared with that of the surrounding liver tissue, which decreased the C/N. Also, some well-differentiated hepatocellular carcinomas retain some hepatocellular function; thus they presumably may take up hepatospecific contrast agents, as has been seen with mangafodipir trisodium (11,25) and Gd-EOB-DTPA (26). In our series, the five well-differentiated hepatocellular carcinomas may have exhibited this hepatocyte-like activity.

Finally, the presence of fat or paramagnetic ions (27) within some types of small hepatocellular carcinomas increases the signal intensity of the lesion on T1-weighted images; thus, on pre- and postcontrast images some hepatocellular carcinomas may have higher signal intensity than the surrounding normal liver tissue. Consequently after administration of Gd-BOPTA, the increased signal intensity in the peritumoral liver parenchyma, as a result of uptake of the contrast agent, may reduce the difference in the signal intensity of the lesion and the normal tissue, and the C/N may be decreased.

The number of primary malignancies identified that were 1 cm or less in diameter did not significantly increase on Gd-BOPTA-enhanced MR images compared with contrast-enhanced CT and unenhanced MR images. Moreover, the difference in the total number of primary lesions identified on MR images compared with the standard of reference was significant on only SE T1-weighted images obtained before and at 40 minutes after administration of Gd-BOPTA;

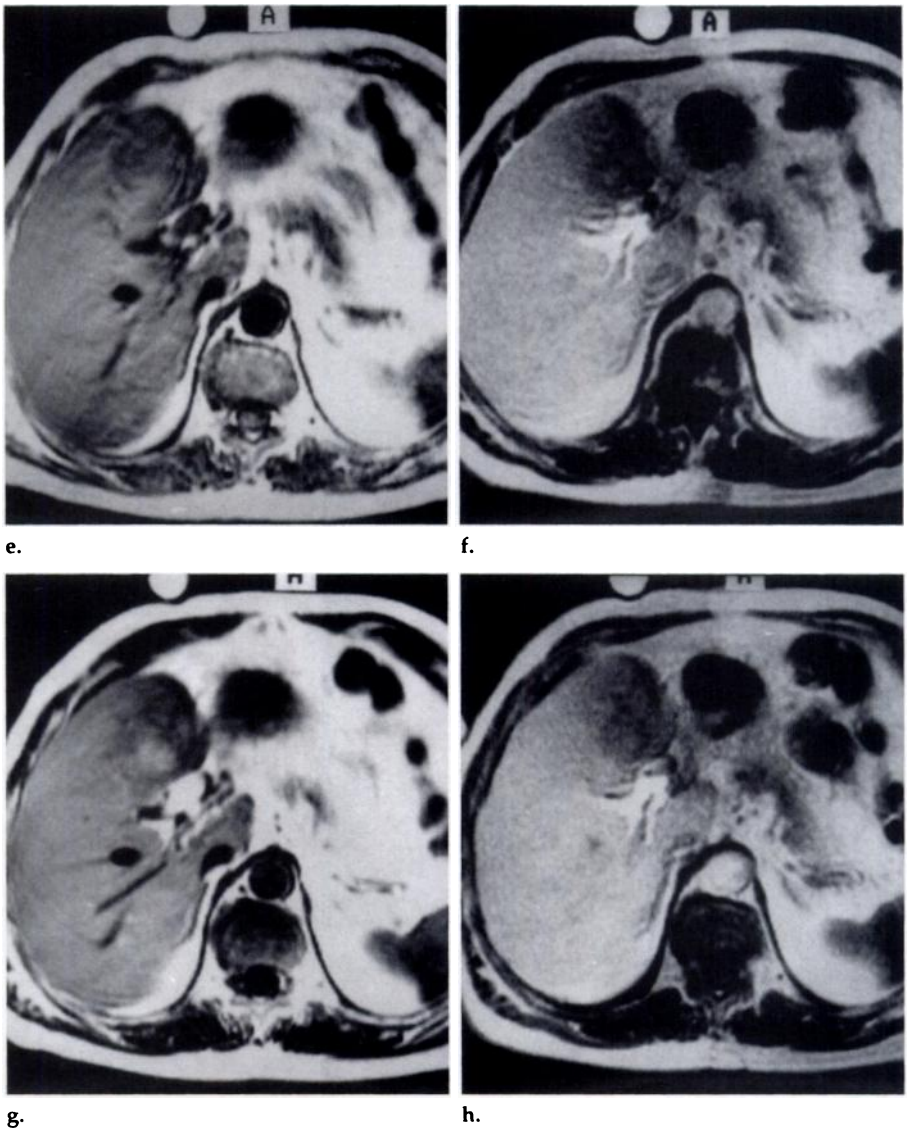

Figure 4 (*continued*). **(e–h)** MR images were obtained at 40 minutes (in **e**, **f**) and 90 minutes (in **g**, **h**) after injection of 0.10 mmol/kg Gd-BOPTA. The images were obtained with conventional SE T2-weighted (in **b**) and T1-weighted (in **c**, **e**, **g**) sequences and with a fast GRE T1-weighted sequence (in **d**, **f**, **h**). The enhancement in the liver parenchyma increased but the C/N of the lesion did not significantly increase on **e–h**.

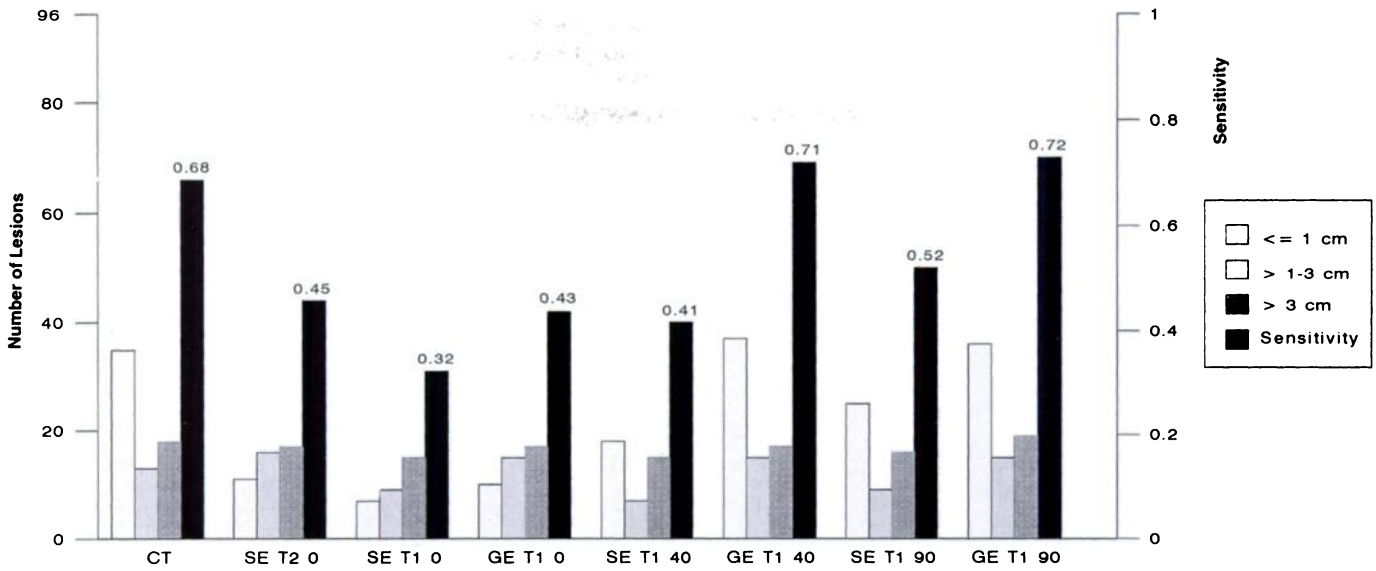

Figure 5. Primary malignant tumors (n = 21). Graph depicts the number of lesions according to size. Sensitivity values (over black bars) refer to the total number of lesions (n = 96) identified at intraoperative US and surgical exploration (standard of reference). Data are presented for lesions more than 1 cm to 3 cm and more than 3 cm in diameter, respectively, throughout. The number of lesions depicted on contrast-enhanced CT (*CT*) scans was 35, 13, and 18, respectively. The number of lesions depicted on precontrast SE (*SE*) T2 (*T2*)-weighted images was 11, 16, and 17, respectively; on precontrast SE T1 (*T1*)-weighted images was seven, nine, and 15, respectively; and on precontrast GRE (*GE*) T1-weighted images was 10, 15, and 17, respectively. The number of lesions depicted on Gd-BOPTA-enhanced SE T1-weighted images at 40 (*40*) minutes was 18, seven, and 15, respectively, and at 90 (*90*) minutes was 25, nine, and 16, respectively; on Gd-BOPTA-enhanced GRE T1-weighted images at 40 minutes was 37, 15, and 17, respectively, and at 90 minutes was 36, 15, and 19, respectively.

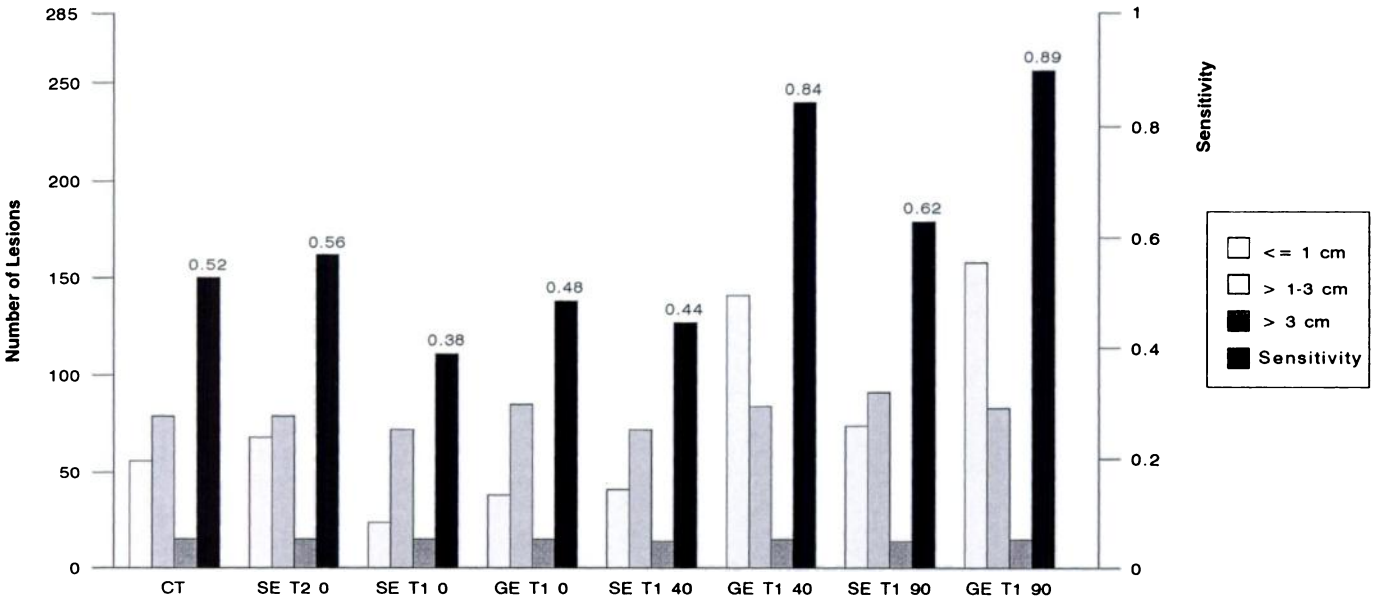

Figure 6. Metastases (n = 13). Graph depicts the number of the lesions identified according to their size. Sensitivity values (over black bars) refer to the total number of lesions (n = 285) identified with intraoperative US and surgical exploration (standard of reference). Data are presented for lesions more than 1 cm to 3 cm or more than 3 cm in diameter, respectively, throughout. The number of lesions depicted on contrast-enhanced CT (*CT*) scans was 56, 79, and 15, respectively. The number of lesions depicted on precontrast SE (*SE*) T2 (*T2*)-weighted images was 68, 79, and 15, respectively; on precontrast SE T1 (*T1*)-weighted images was 24, 72, and 15, respectively; and on precontrast GRE (*GE*) T1-weighted images was 38, 85, and 15, respectively. The number of lesions depicted on Gd-BOPTA-enhanced SE T1-weighted images at 40 (*40*) minutes was 41, 72, and 14, respectively, and at 90 (*90*) minutes was 74, 91, and 14, respectively; on Gd-BOPTA-enhanced GRE T1-weighted images at 40 minutes was 141, 84, and 15, respectively, and at 90 minutes was 158, 83, and 15, respectively.

therefore, Gd-BOPTA may not improve the sensitivity of detection of primary malignancies. Sensitivity values increased the most for contrast-enhanced GRE T1-weighted imaging performed at 90 minutes, although the difference compared with the sensitivity of contrast-enhanced CT was only slight.

The changes in C/Ns were different for liver metastases, because these lesions have no specific cellular uptake of the contrast agent. In the late intervals after administration of Gd-BOPTA, therefore, metastases did not show any important enhancement in most cases, especially not on contrast-enhanced GRE T1-weighted images. Lesion conspicuity was best on these images compared with those obtained with the other sequences, thanks to the great re-

duction in breath- and peristalsis-related artifacts, which improved the identification of lesions 1 cm or less in diameter (Fig 3). Sensitivity values increased the most on contrast-enhanced GRE T1-weighted images obtained at 40 and 90 minutes.

Qualitative analysis in our study indicated that sensitivity improved for Gd-BOPTA-enhanced GRE T1-weighted images, but our study was limited by the lack of independent read-out sessions for pre- and post-contrast MR images. On the other hand, quantitative analysis in our study indicated that results with GRE T1-weighted images obtained with the higher dose of Gd-BOPTA at 90 minutes were significantly superior to results with the unenhanced images obtained with the same sequence. The imaging window provided by Gd-BOPTA, between 40 and 90 minutes, is much longer than the imaging window provided by gadopentetate dimeglumine, which is limited to the early phase of the vascular and interstitial distribution of the contrast agent (2 minutes) (28).

In conclusion, results in this study indicate that intravenously administered Gd-BOPTA is well tolerated by patients. Gd-BOPTA provides a prolonged plateau of signal intensity enhancement within the liver parenchyma, which is greatest with the higher dose of 0.10 mmol/kg, owing to its hepatobiliary specificity. These results are encouraging and optimistic, but more data on the tolerance for and performance of Gd-BOPTA will be available from other clinical trials that are currently under way. ■

References

1. Heiken JP, Weyman PJ, Lee JKT. Detection of focal hepatic masses: prospective evaluation with CT, delayed CT, CT during arterial portography, and MR imaging. Radiology 1989; 171:47–51.
2. Reinig JW, Dwyer AJ, Miller DL, et al. Liver metastasis detection: comparative sensitivity of MR imaging and CT scanning. Radiology 1987; 162:43–47.
3. Stark DD, Wittenberg J, Butch RJ, Ferrucci JT. Hepatic metastases: a randomized, controlled comparison of detection with MR and CT. Radiology 1987; 165:399–406.
4. Nelson RC, Chezmar JL, Sugarbaker PH, Bernardino ME. Hepatic tumors: comparison of CT during arterial portography, delayed CT, and MR imaging for preoperative evaluation. Radiology 1989; 172:27–34.
5. Nazarian LN, Wechsler RJ, Grady CK, et al. CT done 4–6 hr after CT arterial portography: value in detecting hepatic tumors and differentiating from other hepatic perfusion defects. AJR 1994; 163:851–855.
6. Elizondo G, Fretz CJ, Stark DD, et al. Preclinical evaluation of Mn-DPDP: new paramagnetic hepatobiliary contrast agent for MR imaging. Radiology 1991; 178:73–78.
7. Lim KO, Stark DD, Leese PT, et al. Hepatobiliary MR imaging: first human experience with Mn-DPDP. Radiology 1991; 178: 79–82.
8. Hamm B, Vogl TJ, Branding G, et al. Focal liver lesions: MR imaging with Mn-DPDP–initial clinical results in 40 patients. Radiology 1992; 182:167–174.
9. Bernardino ME, Young SW, Lee JKT, Weinreb JC. Hepatic MR imaging with Mn-DPDP: safety, image quality, and sensitivity. Radiology 1992; 183:53–58.
10. Kreft BP, Tanimoto A, Baba Y, Zhao L, Finn JP, Stark DD. Enhanced tumor detection in the presence of fatty liver disease: cell-specific contrast agents. JMRI 1994; 4:337–342.
11. Rofsky NM, Weinreb JC, Bernardino ME, Young SW, Lee JK, Noz ME. Hepatocellular tumors: characterization with Mn-DPDP-enhanced MR imaging. Radiology 1993; 188:53–59.
12. Schumann-Gianpieri G, Schmitt-Willich H, Press WR, Negishi C, Weinmann HJ, Speck U. Preclinical evaluation of Gd-EOB-DTPA as a contrast agent in MR imaging of the hepatobiliary system. Radiology 1992; 183:59–64.
13. Muhler A, Clement O, Vexler V, et al. Hepatobiliary enhancement with Gd-EOB-DTPA: comparison of spin-echo and STIR imaging for detection of experimental liver metastases. Radiology 199; 184:207–213.
14. Hamm B, Staks T, Muhler A, et al. Phase I clinical evaluation of Gd-EOB-DTPA as a hepatobiliary contrast agent: safety, pharmacokinetics and MR imaging. Radiology 1995; 195:785–792.
15. Vittadini G, Felder E, Tirone P, Lo Russo V. B-19036, a potential contrast agent for MR proton imaging. Invest Radiol 1988; 23(suppl 1):S246–S248.
16. Pavone P, Patrizio G, Buoni C, et al. Comparison of Gd-BOPTA with Gd-DTPA in MR imaging of rat liver. Radiology 1990; 176:61–64.
17. Lo Russo V, Pirovano G, Tirone P, Rosati G. Pharmacokinetics and tolerance of Gd-BOPTA/dimeg (abstr). JMRI 1992; 2(P): S18–S19, P233.
18. Vogl T, Pegios W, McMahon C, et al. Gadobenate dimeglumine: a new contrast agent for MR imaging—preliminary evaluation in healthy volunteers. AJR 1992; 158: 887–892.
19. Felder E, Uggeri F, Fumagalli L, Vittadini G, inventors. Bracco International B. V., Amersterdam, The Netherlands, assignee. Paramagnetic chelates useful for NMR imaging. US patent 4,916,246. 1990 Apr 10. Int Cl CO7F 13/00, CO7F 10.02.19236A/86. 1986 Jan 30.
20. Felder E, Fumagalli L, Uggeri F, Vittadini G, inventors. Bracco S. p. A., Milan, Italy, and Bracco International B. V., Amsterdam, The Netherlands, assignee. Paramagnetic chelates. European patent 0 230 893 B1. 1990 June 13. Int Cl CO7C 229/46, CO7C 233/10, CO7C 229/40, CO7D 401/12. IT 1923686. 1986 Jan 30.
21. Stark DD, Wittenberg J, Edelman RR, et al. Detection of hepatic metastases: analysis of pulse sequence performance in MR imaging. Radiology 1986; 159:365–370.
22. Schumann-Gianpieri G. Liver contrast media for magnetic resonance imaging: interrelations between pharmacokinetics and imaging. Invest Radiol 1993; 28:753–761.
23. Cavagna F, Tirone P, Felder E, de Haèn C. Hepatobiliary contrast agents for MRI. In: Ferrucci JT, Stark DD, eds. Liver imaging: current trends and new techniques. Boston, Mass: Andover Medical, 1990; 384–393.
24. Mahfouz AE, Hamm B, Wolf KJ. Peripheral washout: a sign of malignancy on dynamic gadolinium-enhanced MR images of focal liver lesions. Radiology 1994; 190:49–52.
25. Ni Y, Marchal G, Zhang X, et al. The uptake of manganese dipyridoxaldiphosphate by chemically induced hepatocellular carcinoma in rats: a correlation between contrast-media-enhanced magnetic resonance imaging, tumor differentiation, and vascularization. Invest Radiol 1993; 28:520–528.
26. Ni Y, Marchal G, Yu J, Muhler A, Lukito G, Baert AL. Prolonged positive contrast enhancement with Gd-EOB-DTPA in experimental liver tumor: potential value in tissue characterization. JMRI 1994; 4:355–363.
27. Ebara M, Watanabe S, Kita K, et al. MR imaging of small hepatocellular carcinoma: effect of intratumoral copper content on signal intensity. Radiology 1991; 180:617–621.
28. Hamed MM, Hamm B, Ibrahim ME, et al. Dynamic MR imaging of the abdomen with gadopentetate dimeglumine: normal enhancement patterns of the liver, spleen, stomach and pancreas. AJR 1992; 158:303–307.